Short-Term Desensitization of Muscarinic K^+ Current in the Heart

Shingo Murakami,[†‡]* Atsushi Inanobe,[†‡] and Yoshihisa Kurachi[†‡]*

[†]Division of Molecular and Cellular Pharmacology, Department of Pharmacology, Graduate School of Medicine, and [‡]The Center for Advanced Medical Engineering and Informatics, Osaka University, Osaka, Japan

Appendix Figure Legends

Appendix Figure 1. Simulated [$G_{\beta\gamma}$]-dependent activation and current–voltage relationship of the constructed K_{ACh} channel model

(A) [$G_{\beta\gamma}$]-dependent activation of the constructed K_{ACh} channel model. Relative channel availabilities (relative NP_os) of $K_{ACh/high}$ channel (solid line) and $K_{ACh/low}$ channel (dashed line) are calculated by using Eqs. 1 and 2 and compared with that from inside-out patch measurements with a rat atrial myocyte membrane (38) (dotted line).

(B) The current–voltage relationship of I_{KACh} in the constructed K_{ACh} channel model. The current–voltage dependent part in Eq. 2 is shown with experimental I_{KACh} in guinea pig atrial myocytes (1) (filled circles).

Appendix Figure 2. Effects of changes in low affinities of K_{ACh} channel and m2R on short-term desensitization

(AB) Effect of changes in low affinity of K_{ACh} channel on dose-response curves for ACh-induced peak and quasi-steady I_{KACh}. The simulated peak current (I_P) and quasi-steady-state current (I_S) are shown as gray lines for control (K_D for $K_{ACh/low}$ channel is tripled from K_D for $K_{ACh/high}$ channel), red lines in (A) for doubled K_D for $K_{ACh/low}$ channel and blue lines in (B) for sextuple K_D for $K_{ACh/low}$ channel. Experimental data (2) for peak and quasi-steady I_{KACh} are shown as circles with standard deviation [SD]. In the graph, the quasi-steady I_{KACh} induced by 100 μM ACh is expressed as 1.

(CD) Effect of changes in low affinity of m_2R on dose-response curves for I_P and I_S. The same as in (AB) except red lines in (C) are for ten-fold K_D for m_2R and blue lines in (D) for thousand-fold K_D for m_2R.

Appendix Figure 3. [AR·G-GDP] and [AR·G-GTP] during short-term desensitization

Concentrations of G-proteins of nucleotide-bound states before and after GDP/GTP exchange ((ACEGI) for [AR·G-GDP] and (BDFHJ) for [AR·G-GTP] in) are shown for the same simulation conditions in Figure 5.

(AB) Traces of [AR·G-GDP] and [AR·G-GTP] elicited by 200 μM GTP. GTP was applied in the same way as in Fig. 5A. The bar above the traces represents the period of GTP perfusion. The arrowheads indicate the zero level of each trace.

(CD) Effect of 1 mM GDP. As done in Fig 5B, [AR·G-GDP] and [AR·G-GTP] were simulated in the same way as in (AB) except that 1 mM GDP was applied during the entire simulation period.

(EF) Traces of simulated [AR·G-GDP] and [AR·G-GTP] with low receptor expression. As done in Fig 5C, [AR·G-GDP] and [AR·G-GTP] were calculated in the same way as in (AB) except that $[R_H]$ and $[R_L]$ were lowered to 50%.

(GH) Effect of high GDP/GTP exchange activity on [AR·G-GDP] and [AR·G-GTP]. As done in Fig 5D, GDP/GTP exchange was enhanced by increasing the rate constants for GDP/GTP exchange by a factor of 5. The period during which ACh was perfused is shown as a bar above the trace.

(IJ) The effect of low GDP/GTP exchange activity on [AR·G-GDP] and [AR·G-GTP]. As done in Fig 5E, GDP/GTP exchange was lowered by reducing the rate constants to one-half.

Appendix Figure 4. Sensitivity of the maximum conductance of the K_{ACh} channel to asystole length

The effects of maximum conductance of the K_{ACh} channel on asystole length with 10 μM [ACh] are calculated for the (A) Demir and (B) Kurata sinoatrial node models. Only results

obtained when sinus rhythms were resumed are shown as lines. The cross marks correspond to the simulation conditions in Figure 7.

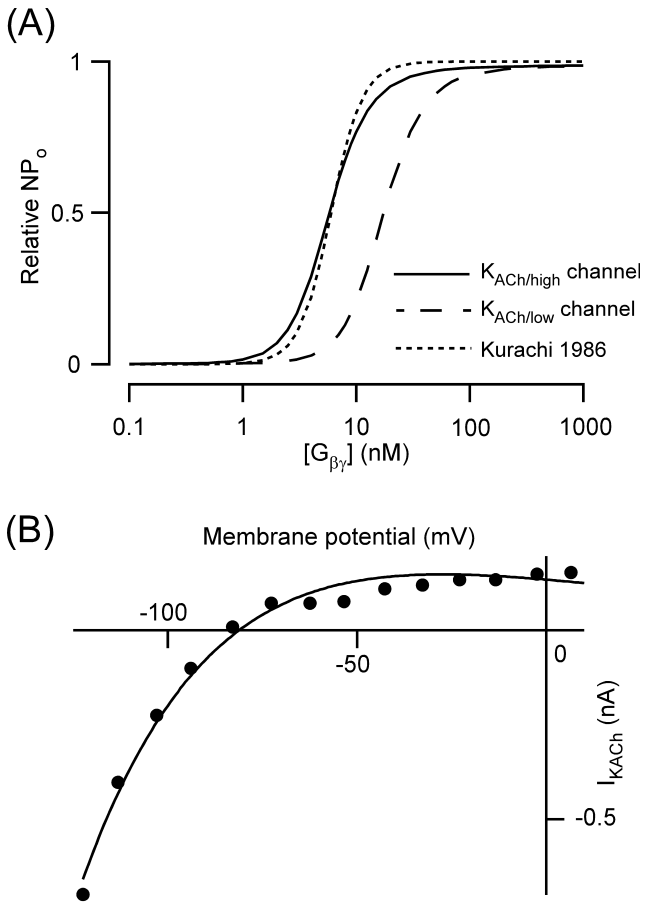

Appendix Fig. 1 Murakami et al.

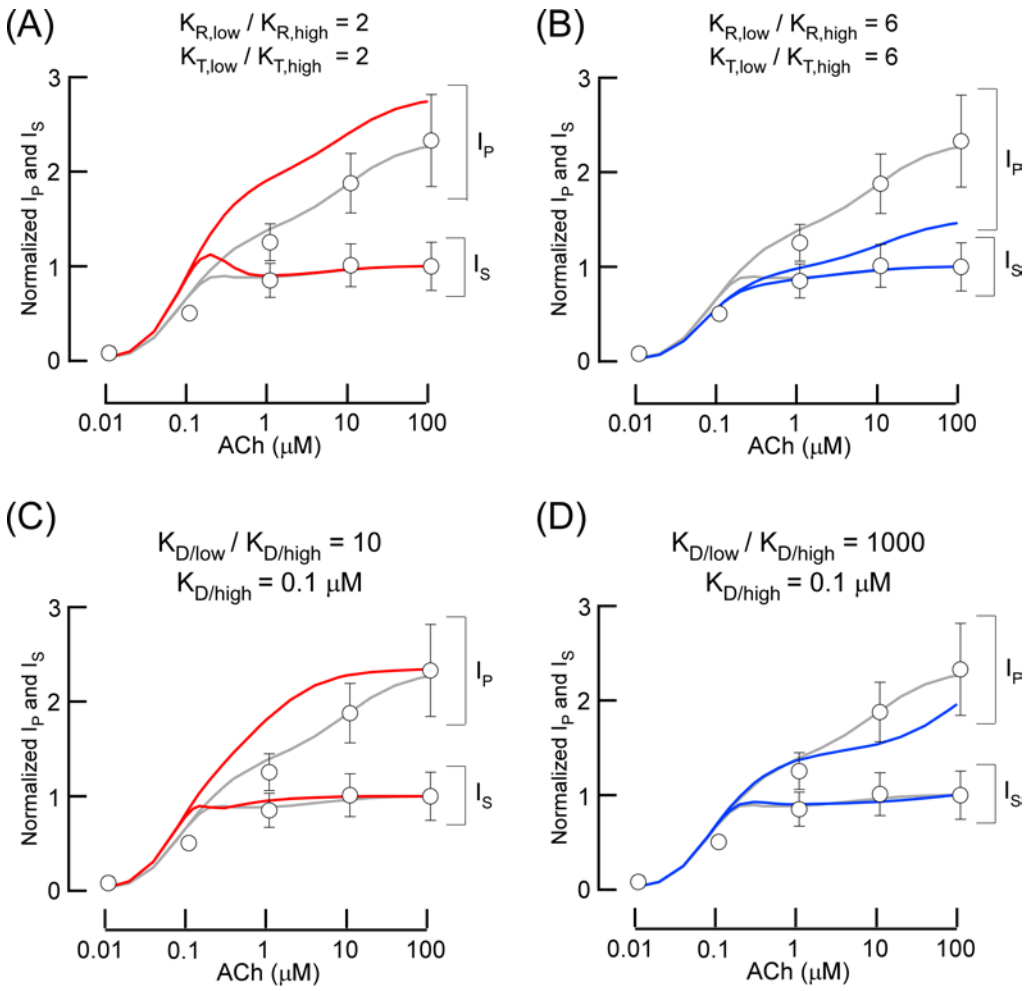

Appendix Fig. 2 Murakami et al.

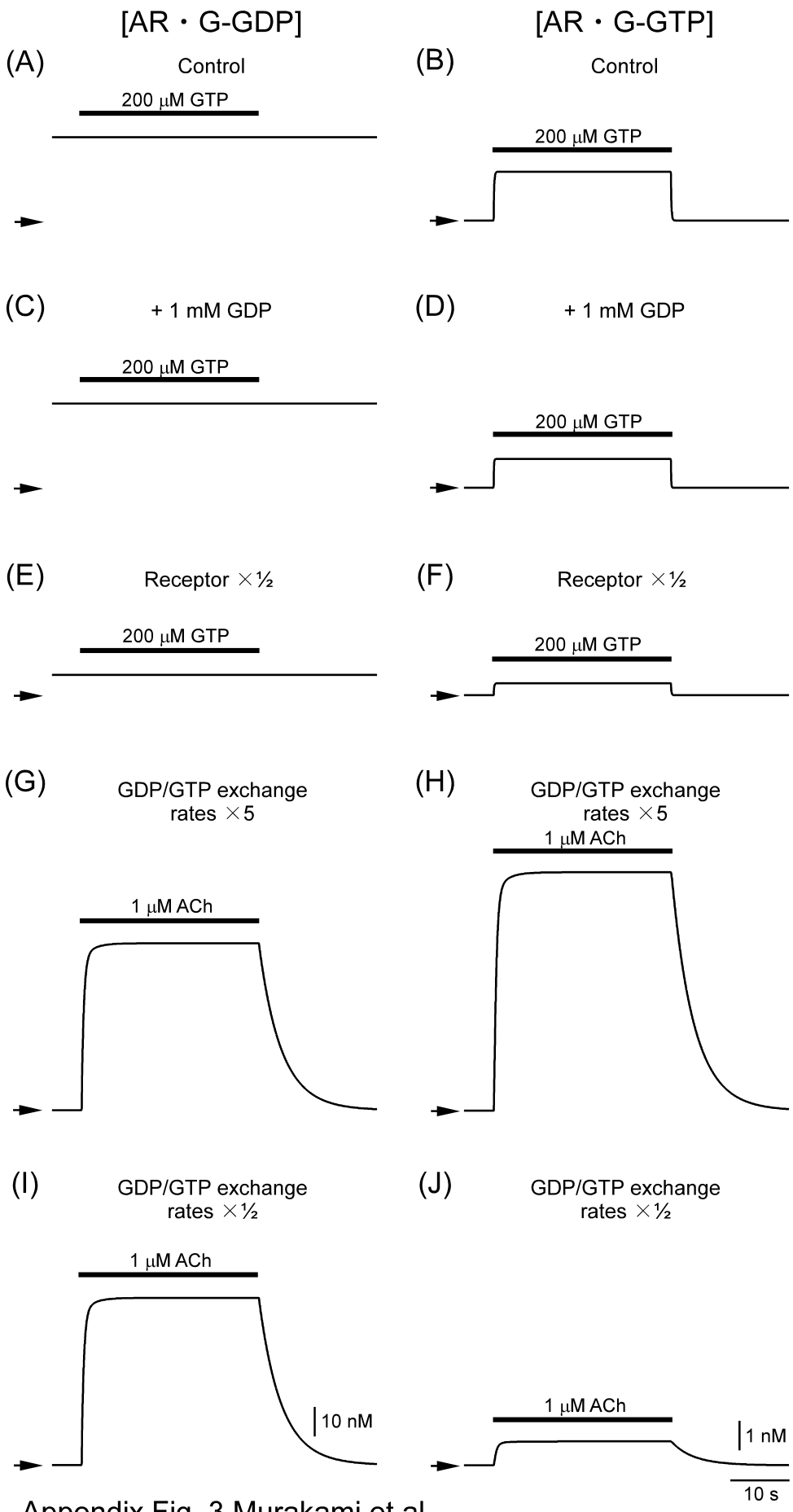

Appendix Fig. 3 Murakami et al.

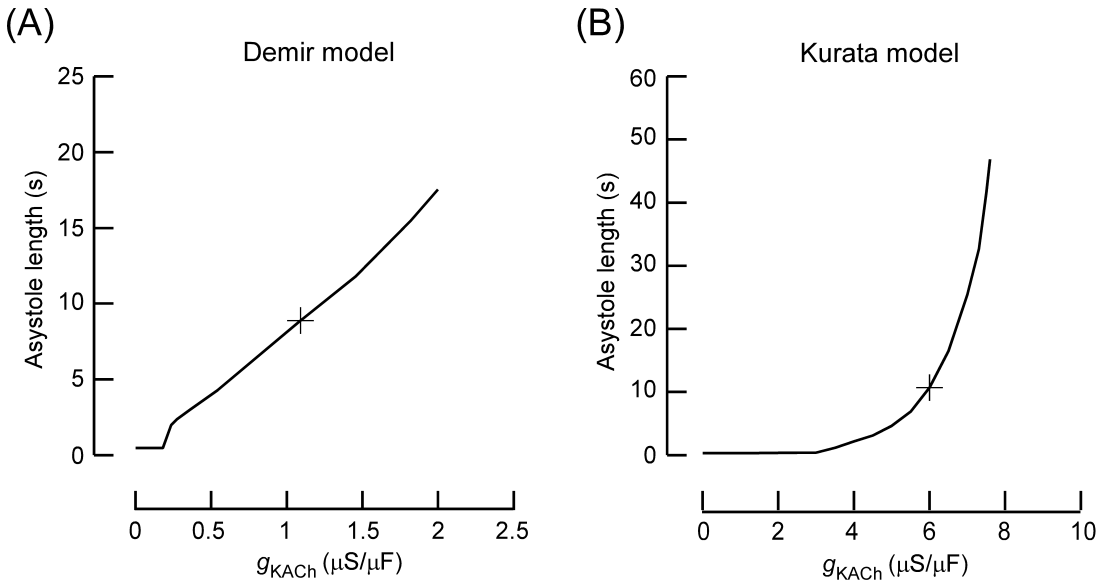

Appendix Fig. 4 Murakami et al.